

Supporting Information

MoS₂ Encapsulated in Three-Dimensional Hollow Carbon

Frameworks for Stable Anode of Sodium Ions Batteries

Min Liu,^{a, b} Sihan Chen,^{a, b} Ying Jin,^{, c} and Zhen Fang^{*, a, b, d}*

^a College of Chemistry and Materials Science, Key Laboratory of Electrochemical Clean Energy of Anhui Higher Education Institutes, Anhui Normal University, Wuhu, 241002, P. R. China.

^b Key Laboratory of Functional Molecular Solids, Ministry of Education, Anhui Normal University, Wuhu, 241002, P. R. China.

^c School of Chemical and Environmental Engineering, Anhui Polytechnic University, Wuhu, 241002, P. R. China.

^d Anhui Provincial Engineering Laboratory for New-Energy Vehicle Battery Energy-Storage Materials, Wuhu, 241002, P. R. China.

*Corresponding author, Ying Jin: daylilyjin@163.com, Zhen Fang: fzfsnc@mail.ahnu.edu.cn. TEL./Fax, +86-553-3869302

Experimental Section

Chemicals and reagents

Sodium molybdate ($\text{Na}_2\text{MoO}_4 \cdot 2\text{H}_2\text{O}$), corn starch, thiourea ($\text{CH}_4\text{N}_2\text{S}$), Polyvinylpyrrolidone($(\text{C}_6\text{H}_9\text{NO})_n$, Average molecular weight: 58000)

were purchased from Aladdin Industrial Co., Ltd (Shanghai, China). Sodium hydroxide (NaOH) were purchased from Sinopharm Chemical Reagent Co., Ltd (Shanghai, China). Polyethylene glycol-10000($\text{HO}(\text{CH}_2\text{CH}_2)_n\text{H}$, Average molecular weight: 8500-11500) was purchased from Xilong Chemical Co., Ltd(Guangdong, China).

Material characterization

The phase and crystal structure of the product were studied by Bruker D8-Advanced X-ray Diffractometer ($\text{Cu K}\alpha$ radiation, 40 kV, 40 mA), scanning electron microscopy (SEM, Hitachi S-4800, 5 kV) were used to characterize the surface morphology of the material. Transmission electron microscopy (TEM, FEITECNAI-G2 200 kV) was determined to obtained the microstructure of the material. High-resolution transmission electron microscopy (HRTEM) analyses were carried out on a FEI TECNAI-G2 microscope with an accelerating voltage of 200 kV. The elemental composition and valence state of the samples were analyzed by X-ray photoelectron spectroscopy (XPS, ESCALAB Perkin Elmer). Raman spectra were tested by a Renishaw's Invia Raman microscope and N_2 adsorption-desorption measurements were determined by ASAP 2460 (micromeritics).

Electrochemical measurements

The CR2032 coin cells was used to conduct electrochemical tests on $\text{MoS}_2@\text{HCF}$ composite materials prepared with different carbon sources.

The active material, carbon black (acetylene black) and binder (polymethylcellulose sodium) are mixed in a mass ratio of 6:2:2 to prepare a working electrode, which is evenly spread on copper foil and cut to the same size electrode sheet, and dried at 60 °C for 12 overnight at vacuum oven. The 1.0 M NaClO₄ electrolyte which is composed of ethylene carbonate (EC)/diethyl carbonate (DEC) (volume 1:1) and 5 % vinyl fluoride carbonate (FEC) used to assemble the battery. A battery tester (Newark, Shenzhen, China) was used to test the battery performance at a voltage window from 0.01 ~ 3.0 V. With the help of CHI-660E electrochemical workstation, we successfully obtained cyclic voltammetry (CV) and electrochemical impedance spectroscopy (EIS). The thermogravimetric (TGA) analysis of the product collected by the SDT 2960 under the air atmosphere of 800 °C with a programmed temperature of 10 °C/min.

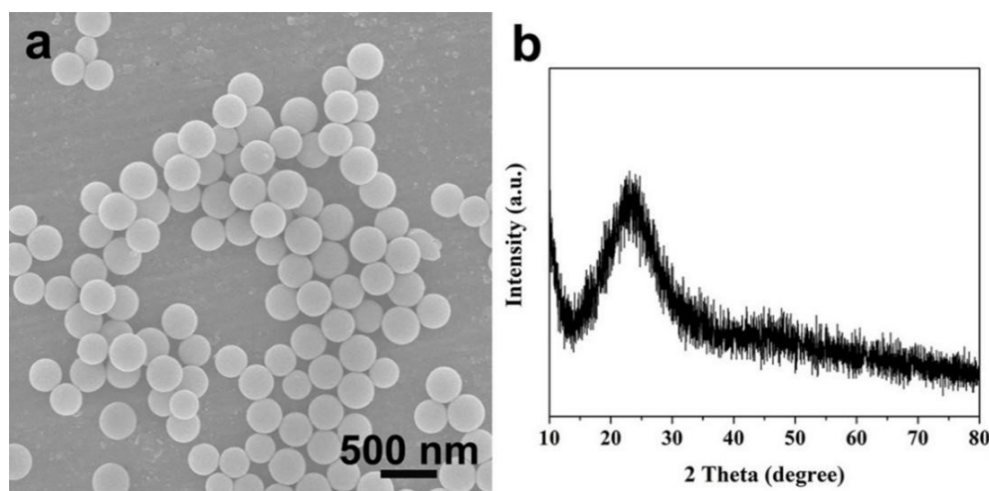


Fig. S1 SEM images of (a) SiO_2 , (b) XRD pattern of SiO_2 .

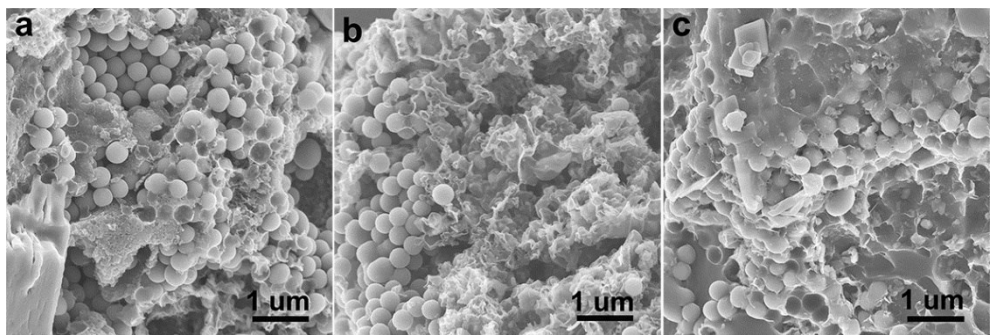


Fig. S2 SEM images of calcined precursor: (a) $\text{MoO}_4^{2-}/\text{SiO}_2@\text{PVP-C}$.
(b) $\text{MoO}_4^{2-}/\text{SiO}_2@\text{PEG-C}$, (c) $\text{MoO}_4^{2-}/\text{SiO}_2@\text{Starch-C}$.

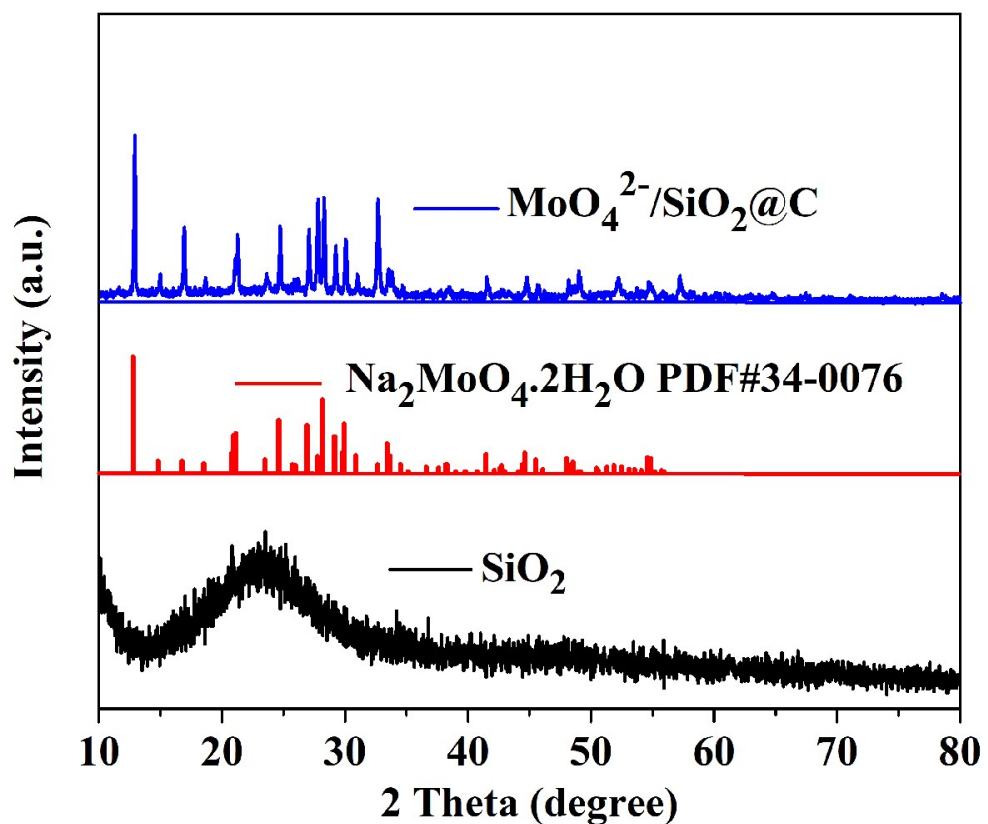


Fig. S3 XRD pattern of $\text{MoO}_4^{2-}/\text{SiO}_2@\text{C}$.

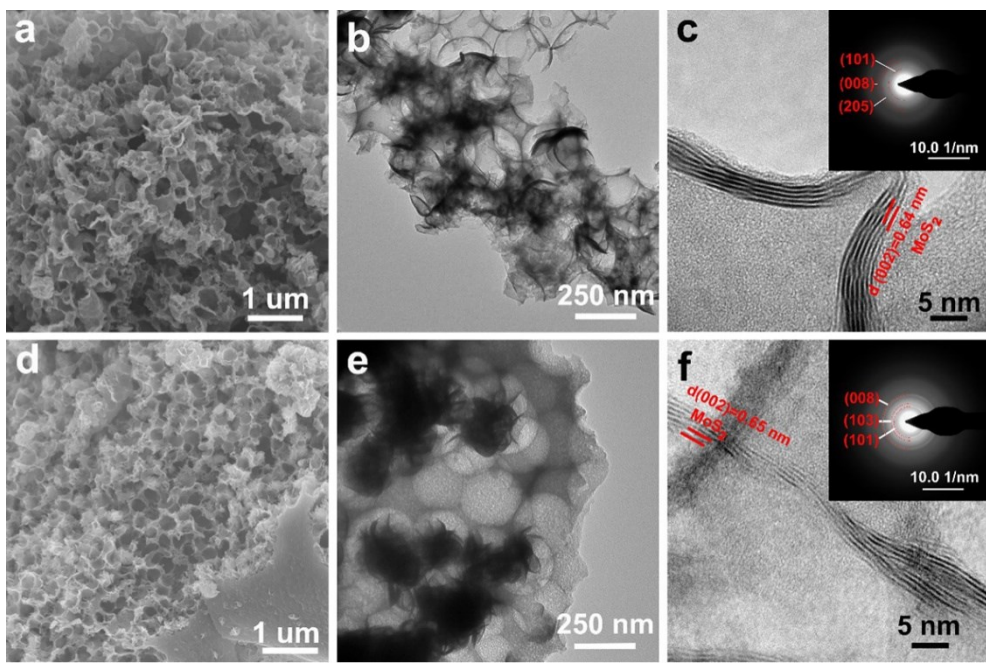


Fig. S4 (a-c) SEM, TEM HRTEM and SAED images of MoS₂@PEG-HCF, (d-f) SEM, TEM HRTEM and SAED images of MoS₂@Starach-HCF.

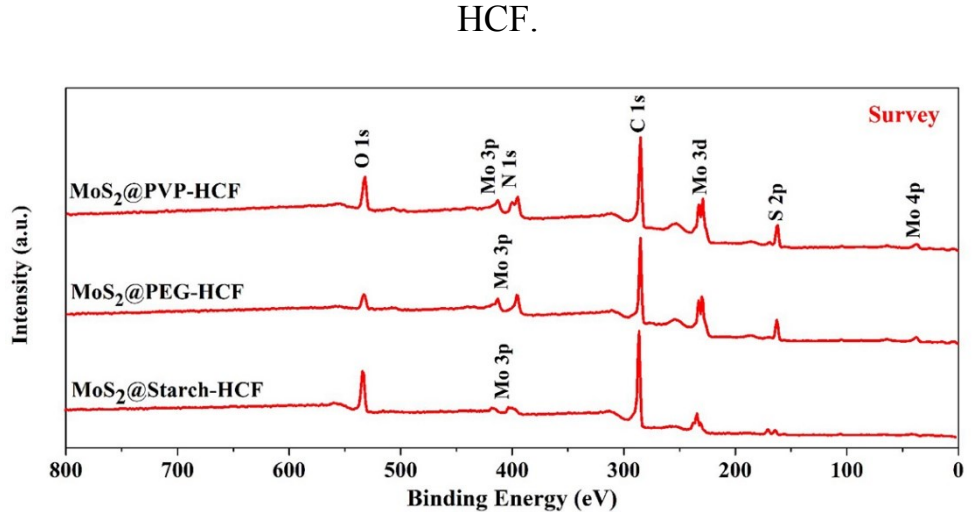


Fig. S5 The integrated XPS spectrum of MoS₂@HCF with different carbon sources.

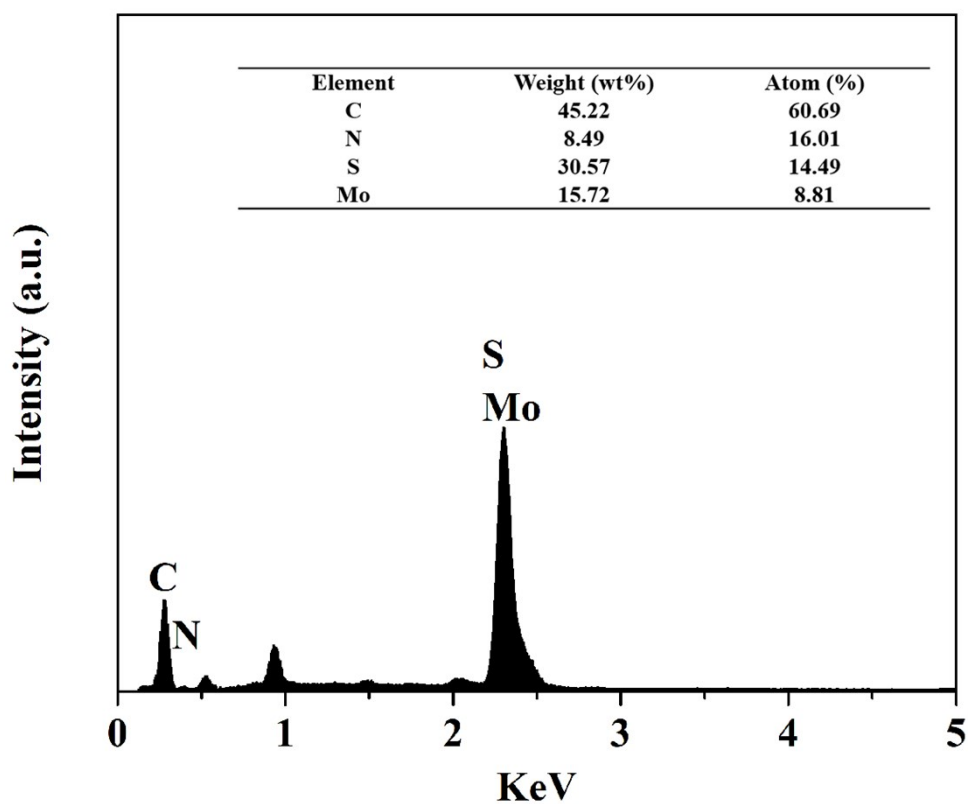


Fig. S6 The EDX results about the content of each element in $\text{MoS}_2@\text{PVP-HCF}$ composite.

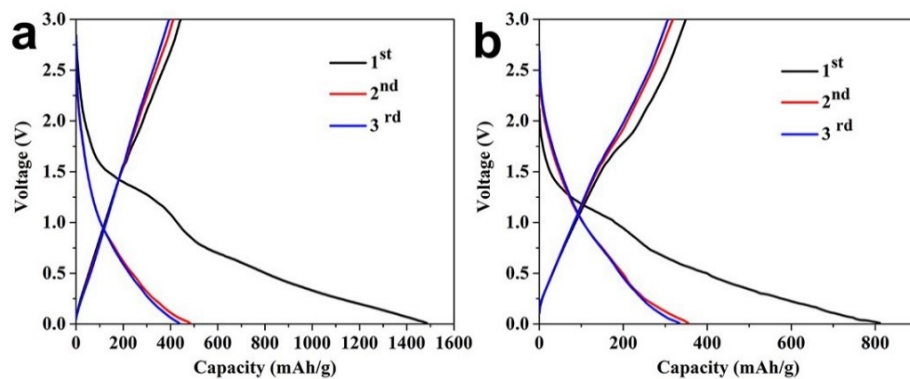


Fig. S7 The discharge and charge profiles of $\text{MoS}_2@\text{Starch-HCF}$ and $\text{MoS}_2@\text{PEG-HC}$ in the initial 3 cycles at a current density of 50 mA g^{-1} .

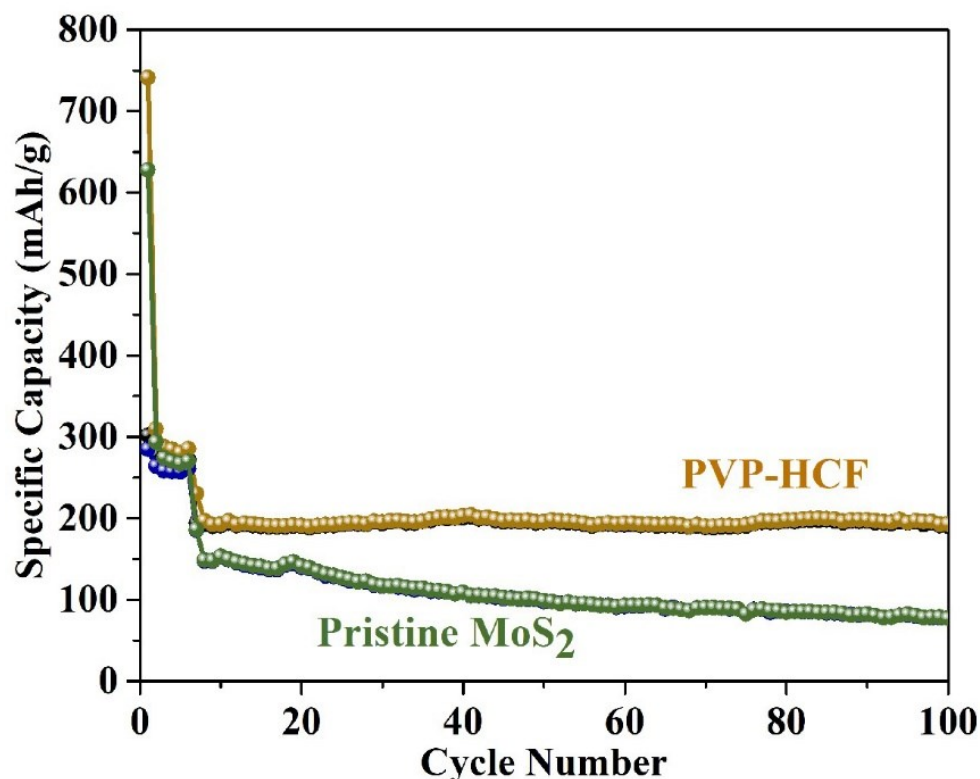


Fig. S8 Cycling performances of pure MoS₂, and HCF-PVP at 0.1 A

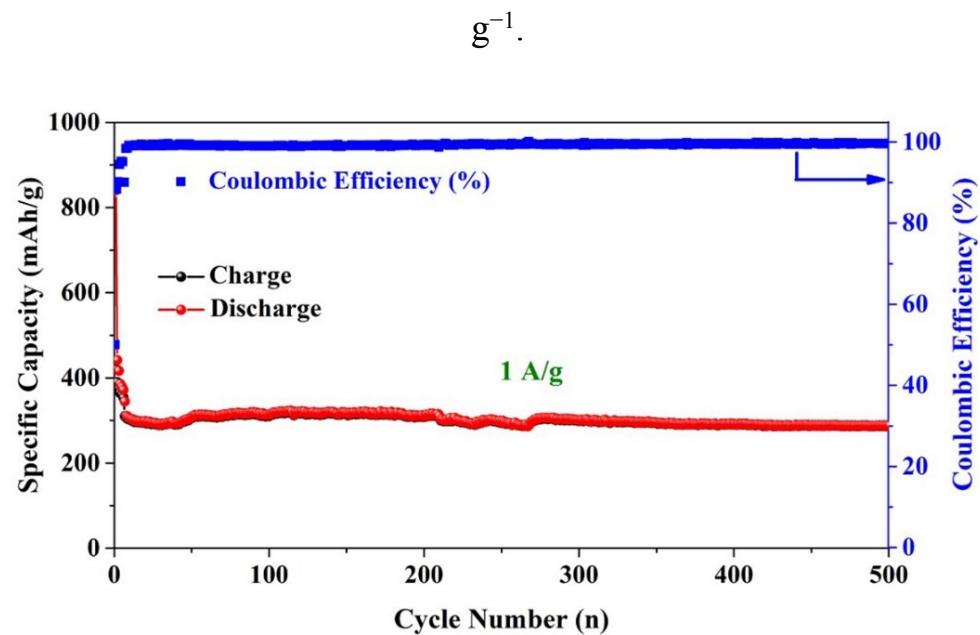


Fig. S9 Cycling performances of MoS₂@PVP-HCF at 1A g⁻¹ for 500 cycles.

Table S1 Comparison of SIBs performances of MoS₂@C in this work and other literatures.

Electrode materials	Current density (A g ⁻¹)	Discharge capacity (mA h g ⁻¹)	Cycles	Reference
MoS ₂ @C	2	225	400	This work
MoS ₂ /MoO ₃ /C	1	339	220	¹
Mn-MoS ₂	0.1	441	200	²
S/MoS ₂	0.5	302	300	³
MoS ₂ /C	0.1	447	100	⁴
MoS ₂ /C	1	319	1500	⁵
MoS ₂ -GC	0.5	542	250	⁶
MoS ₂ -RGO	0.1	305	50	⁷
MoS ₂ @AMCRs	1	305	300	⁸
MoS ₂ @CNFs	0.1	528	100	⁹
MS-RGO	0.1	372	50	¹⁰
Fe ₃ O ₄ @MoS ₂ -GP	0.1	388	300	¹¹
MoS ₂ -rGO/HCS	1	443	500	¹²
RGO/MoS ₂	1	312	600	¹³

Table S2 At a current density of 1 A g⁻¹, the equivalent circuit model is used to simulate the impedance value of the electrode before and after 500 cycles.

Electrode	Rs (Ω)	Rer (Ω)
MoS ₂ @PVP-HCF (before cycle)	4.412	238.8
MoS ₂ @PVP-HCF (after cycle)	4.004	149.8
MoS ₂ @PEG-HCF (before cycle)	7.428	226.3
MoS ₂ @PEG-HCF (after cycle)	4.293	126.0
MoS ₂ @Starch-HCF (before cycle)	8.294	227.6
MoS ₂ @Starch-HCF (after cycle)	6.425	115.6

References

1. K. Zhu, X. Wang, J. Liu, S. Li, H. Wang, L. Yang, S. Liu and T. Xie, *ACS Sustainable Chem. Eng.*, 2017, **5**, 8025-8034.
2. T. Zheng, G. Li, J. Dong, Q. Sun and X. Meng, *Inorg. Chem. Front.*, 2018, **5**, 1587-1593.
3. Z. Xu, K. Yao, Z. Li, L. Fu, H. Fu, J. Li, L. Cao and J. Huang, *J. Mater. Chem. A*, 2018, **6**, 10535-10542.
4. J. Wu, Z. Lu, K. Li, J. Cui, S. Yao, M. Ihsan-Ul Haq, B. Li, Q. H. Yang, F. Kang and F. Ciucci, *J. Mater. Chem. A*, 2018, **6**, 5668-5677.
5. H. Wang, H. Jiang, Y. Hu, P. Saha, Q. Cheng and C. Li, *Chem. Eng.*

Sci., 2017, **174**, 104-111.

6. T. S. Sahu, Q. Li, J. Wu, V. P. Dravid and S. Mitra, *J. Mater. Chem. A*, 2017, **5**, 355-363.
7. W. Qin, T. Chen, L. Pan, L. Niu, B. Hu, D. Li, J. Li and Z. Sun, *Electrochim. Acta*, 2015, **153**, 55-61.
8. Y. Pang, S. Zhang, L. Liu, J. Liang, Z. Sun, Y. Wang, C. Xiao, D. Ding and S. Ding, *J. Mater. Chem. A*, 2017, **5**, 17963-17972.
9. W. Li, R. Bi, G. Liu, Y. Tian and L. Zhang, *ACS Appl. Mater. Interfaces*, 2018, **10**, 26982-26989.
10. J. Li, W. Qin, J. Xie, R. Lin, Z. Wang, L. Pan and W. Mai, *Chem. Eng. J.*, 2018, **332**, 260-266.
11. D. Kong, C. Cheng, Y. Wang, Z. Huang, B. Liu, Y. Von Lim, Q. Ge and H. Y. Yang, *J. Mater. Chem. A*, 2017, **5**, 9122-9131.
12. X. Hu, Y. Li, G. Zeng, J. Jia, H. Zhan and Z. Wen, *ACS Nano*, 2018, **12**, 1592-1602.
13. T. Cheng, J. Xu, Z. Tan, J. Ye, Z. Tao, Z. Du, Y. Wu, S. Wu, H. Ji, Y. Yu and Y. Zhu, *Energy Storage Mater.*, 2018, **10**, 282-290.